Evolution of Tip Vortices Generated by Two Bladed Rotor in Hover at Early Wake Ages

Byung Ho Park* and Yong Oun Han**
School of Mechanical Engineering, Yeungnam University, Gyongsan, Korea

Abstract

In order to investigate change of vortex structures and its evolving processes, two dimensional LDV system was used for measurement of velocity vectors of tip vortex, and PIV system was also used for visualizations of tip vortex array for two bladed rotor, respectively. Experiments provided vortex locations, tangential and axial velocity components of tip vortex at six wake ages of 9.5, 10.5, 60.5, 99.5, 129.5, 169.5 and corresponded six wake ages shifted with 180 degrees per each. It was resulted that tip vortices generated by the first blade satisfy Landgrebe's model for their vortex locations even after they were accelerated by the second blade in downstream. Tangential velocity components of tip vortices follow Vatistas' n=2 model on both inside and outside regions of rotor slipstream without loss of vortex circulation. Axial velocity profiles revealed that there were small but significant perturbations just outside the primary vortex core which implies the second blade affects the wake substantially. It was also found that tip paths of each blade were not willing to be coincided intrinsically.

Key words : helicopter, tip vortex, two bladed rotor, LDV system, visualization

Introduction

Compared to tip vortices and their trails of a fixed airplane, those of helicopter are lingering around the helicopter body and near wakes. Naturally, it is the high induced velocities surrounding the tip vortices that become a source of unsteady aerodynamic forces, and these can be a significant source of rotor noise and airframe vibrations. Therefore, any device which can reduce the strength of tip vortex provides substantial advantages for both improving vehicle stability and reducing rotor noise.

In a hover the vortex trail forms a helical trace with respect to the vertical rotor hub axis, and the slip stream becomes contracted rather drastically within one revolution of rotor blade, making the angular momentum of the tip vortex grow quickly. During a whole life time, tip vortex generally experience namely four different modes of motion; diffusion, dissipation, stretching (or, elongation) and distortion along the vortex trail. After matured, until 14 degrees of wake age reported by Han & Leishman [1], tip vortex experiences diffusion, distortion and stretching during its evolving process. It is known that vortex diffusion and dissipation proceed continuously until disappeared, but distortion and stretching eventuates far downstream with both being correlated. At this stage the helical trace cannot be maintained, and both motions are really difficult to be quantified in wake calculation as well as in experiments.

Jwp aj
* Ph.D. Candidate
** Professor
E-mail : yohan@yu.ac.kr Tel: +82-53-810-2454 Fax: +82-53-813-3703

Understanding the physics of vortex formation, the vortex size, radial distribution of swirl velocity, as well as diffusion and dissipative mechanism, will have a fundamental impact on the ability to predict these metrics and minimize adverse vortex induced effects. An improved understanding of rotor tip vortices is imperative to help understand the aero-acoustic problems associated with blade vortex interaction (BVI) [2, 3] and the large unsteady air-loads produced by rotor wake airframe interactions [4, 5].

A single bladed rotor operated in the hovering state was frequently used to observe basic physics of the tip vortex [6-8]. The single bladed system provides the ability to create and study a helicoidal vortex filament without interference from other vortices generated by other blade, thereby allowing much more spatially and temporally stable tip vortex structure than the multiple blades case. Thereby, it allows to investigate fairly older wake ages characteristics and to be free of the high aperiodicity issues in multi-bladed helicopter rotor experiment. But one bladed rotor system still has limit to observe the distortion and stretching mechanism which appear mostly at older wake ages even through it provides advantages to examine the growing and diffusion of tip vortex in early wake age.

Compared to single bladed rotor system, two bladed rotor provides sophisticate information about vortex distortion as well as diffusion within one revolution of both blades with rather simplicity. This system makes it possible to observe the change of vortex structure effectively by comparing both vortices generated by each blade at same wake ages before and after 180 degrees. It is naturally expected that tip vortex affected by the second blade may experience the distortion earlier including the vortex diffusion. Therefore, instead of investigating a quite old wake aged vortex which is very difficult to examine in most case, substantial change of vortex structure can be obtained by interference of the second blade.

This paper aims primarily to investigate change of vortex structures without and with the second blade effect by the use of experimental devices; two dimensional LDV system for the velocity vector of tip vortex and PIV system for visualization of tip vortex array. These experimental results will be utilized for prediction to diffusion, distortion and stretching of tip vortex basically, thereby providing basic data and allowing tip vortex control eventually to improve the aerodynamic performance and noise issues of helicopter rotor.

Description of the Experiments

A two bladed rotor operated in the hovering state was used for the measurements. Square tip wooden blade was used with the radius of 0.445m and the chord of 0.05m. Blade has the airfoil section of NACA2415, untwisted. Each blade was secured to a teetering fixture at the Aluminum hub which was driven by a three phase constant torque electric motor, capable of reaching an average speed of 2,100rpm in the two blades loaded case, giving a tip Mach number and chord Reynolds number of 0.27 and 2.7 x 10^5, respectively. The collective pitch was set at 4 ° for both blades. The motor was mounted horizontally in a rotor stand to make rotor wake convected away from the rotor plane.

Experiments were basically designed to obtain the vortex location and vortex velocity vectors by use of PIV system and LDV system, respectively. To investigate the vortex location visualization image was obtained by seeding the flow using a mineral oil fog strobbed with a laser sheet. This light sheet was produced by a dual Nd:YAG laser. Images were acquired using a high resolution charge-coupled-device (CCD) camera. More than hundred images were used to find the location of vortex centers by pointing them in a manual way. These center locations tell easily how the rotor slip stream builds up as the wake age grows. Schematic layout of visualization system is shown in figure 1.

Two velocity components of tip vortex, axial and tangential vectors, were measured using a fiber-optic based 2 dimensional LDV system (DANTEC, BSA). This system comprised a 6-W argon-ion laser source (Spectra Physics), beam separators, a matrix of fiber optic coupler, transmitting optics with beam expanders, and coaxial receiving optics.

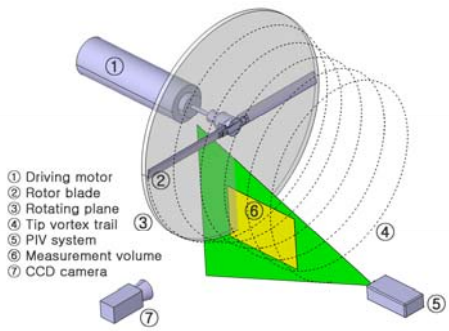

Fig. 1. Experimental set up of rotor and PIV system

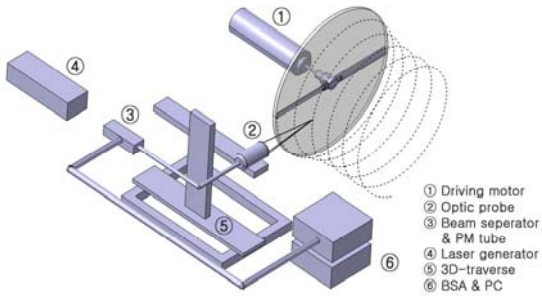

Fig. 2. Rotor disk plane and 2-D LDV system

The four beams (two colors for each velocity component, with one of each pair being frequency shifted) were focused at a point in the rotor wake. The measurement volume was moved by traversing the entire optics package in three orthogonal directions by using a computer controlled traverse (see Fig. 2).

The seed particles used for both velocity measurement and visualization were produced by vaporizing mineral oil into a dense fog. The particle sizes were between 0.2 and 0.22 μm diameter. This mean seed particle size was small enough to minimize particle tracking errors for the vortex strength especially.

Results and Discussions

3.1 Vortex Locations

At a fixed vertical plane of a laser sheet vortex images were captured at various azimuthal angles or, wake ages of rotor by changing pulse interval of sheets. Because of a strong angular momentum the vortex centers cannot keep particles at the center so that they have clear voids by the centrifugal forces. If the closest vortex to the rotating plane was generated by the first blade its next vortex at the same plane is appeared at the third position which is connected by the helical trail because the second vortex was generated by the second blade.

To understand the blade effect for the core location visual images were made by two bladed rotor experiment done with the rotating speed of 2100rpm (tip Mach number = 0.27). The core motion closely related to the rotor wake and the interference with the ensuing blade. It is convenient look over the wake history of one-revolutions of two blades for predicting far wake characteristics. The sequential location of vortices shows that the slip stream was rapidly contracted with a half of rotor revolution as shown in the figure 3. Sequential vortices seem to distribute linearly in downstream once the slipstream contracted at beginning. Also, the vortex array is slightly different from the single case which array is normally curved. It explains that the 2^{nd} blade promotes the vortex trail of the first blade to accelerate in downstream direction.

More than a hundred snap images taken by PIV system were used to gather the center locations by pointing the void centers in a manual way which needs extreme patience. Their results are shown in figure 4.

Vortex locations captured were compared with Landgrebe’ s model [9] such as;

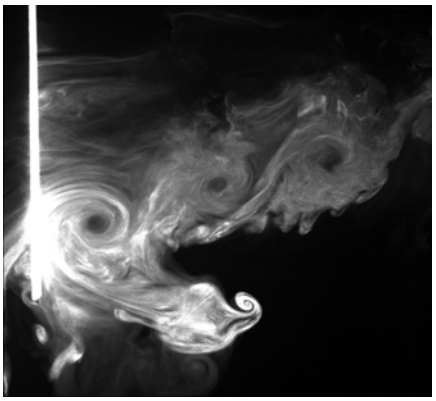

Fig. 3. Flow visualization image of vortex wake generated by two bladed rotor

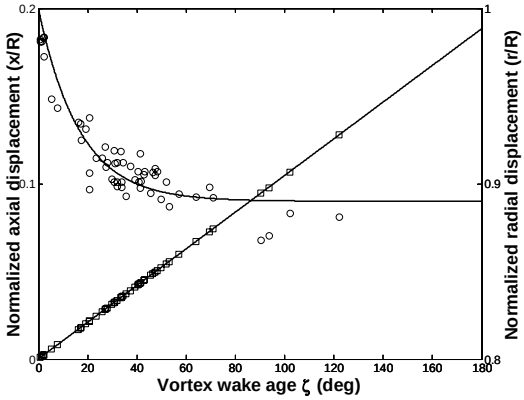

Fig. 4. Normalized vortex locations obtained by using visualization images, and model fits for translation and contraction behaviors

$$\frac{x}{R} = \begin{cases} \kappa_1 \ \zeta & 0 \le \zeta \le \dfrac{2\pi}{N} \\ \left(\dfrac{\zeta}{R}\right)_{\zeta=\frac{2\pi}{N}} + \kappa_2 \left(\dfrac{\zeta - 2\pi}{N}\right) & \zeta \ge \dfrac{2\pi}{N} \end{cases}, \quad \frac{r}{R} = A + (1-A)e^{-\lambda\zeta} \tag{1}$$

where x is axial distance [m], r is radial distance [m], R is rotor radius [m], ζ is wake age [deg], and N is number of blades, respectively. The constant A is an empirical number dependent of the contraction ratio of the slip stream.

By accumulating all vortex locations in the same plot, wake boundary can be established by the Landgrebe' s model equation (1). This model suggested the translation coefficient, $k_1 = 0.0225$ and the contraction rate, $\lambda = 0.23$, respectively.

By using the equation (1) this experimental results were well matched with constants of the tip vortex translation coefficient, $k_1 = 0.02247$ and the contraction coefficient, $\lambda = 0.3103$ for A = 0.78, respectively. Coyne reported similar results of both single blade and two blade cases as shown in both the figure 5 and table 1. Note that values of exponent λ of two bladed cases are bigger than those of one blade cases. It means that the two bladed rotor system has more drastic contraction ratio than the single case in this experimental range of wake age. But as shown in figure 5, compared to radial component, axial displacement was pretty close to those of single blade model.

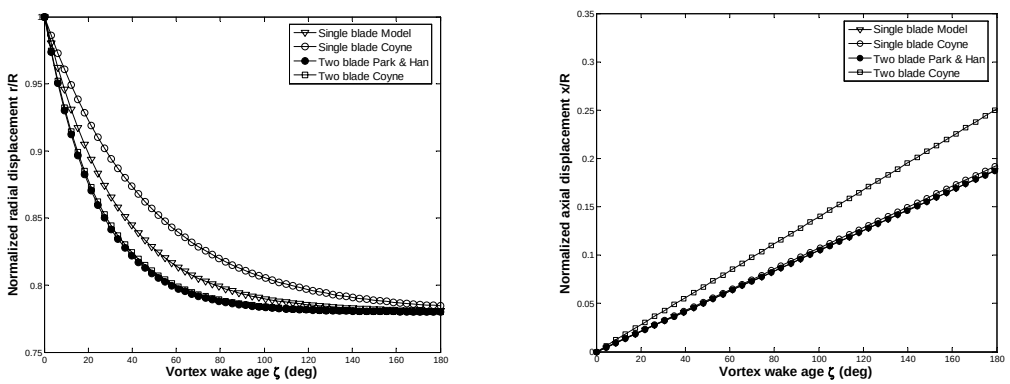

Fig. 5. Comparisons of vortex locations with previous experimental results of single and two bladed cases; contraction (left) and translation (right), respectively

Table 1. Location coefficients

	Single blade system		Two bladed system	
	Model	Coyne	Park & Han	Coyne
K1	0.0225	0.023	0.02247	0.03
λ	0.23	0.16	0.3103	0.3

3.2 Tangential velocities

Velocity vector measurements were carried out at six different wake ages so far at 9.5, 10.5, 60.5, 99.5, 129.5 and 167.5 degrees. Experiments were initially intended to be made at twelve different wake ages, six wake ages before 180 degrees, and corresponded later wake ages shifted with 180 degrees, respectively, to observe the ensuing blade interference. But it was found that to coincide two tip paths of each blade was really difficult so that velocity vectors of each tip vortex were deviated each other which can be seen in the figure 6. If tip path of two blades are exactly coincided, their profiles should be collapsed.

As seen in figures, drastic change of tangential velocity explains that tip vortex has strong angular momentum near the vortex core radii, and that core radius is very small as much as 1% of rotor radius in early stages. It has been reported that tip vortex is growing continuously until about 15 degrees of wake age and starts to diffuse by the viscous dissipations [10]. Based on this observation, the first two cases in the figure 6 shows growing tip vortices.

As wake age grows the vortex center quickly moves toward the rotor hub at the beginning stage as observed in vortex location. Peak value of tangential velocity component can be used to calculate the vortex circulation so that the rough idea of the vortex strength can be estimated. It is of nature that the vortex strength should be decayed because the vortex becomes diffused as wake age. Also the core size provides the diffusing rate. Therefore, vortex velocity vector components and their evolution with wake age inform about diffusion and distortion of tip vortices.

To allow a further analysis of the vortex profile, the convection velocity was removed by subtracting the time averaged flow velocity over one rotor revolution at the same grid points from the phase averaged velocities, thereby leaving a residual velocity field. These data are shown in figure 8. The remaining asymmetry of the vortex profile is because of the self induced effects of curvature and contraction of what is an almost helical filament [11].

The tangential velocity component was generally found to be closely approximated by n =2 case of the series of two-dimensional algebraic profiles given by Vatistas et al [12] as,

$$V(\bar{r}) = \frac{\bar{\Gamma}}{2\pi r_c}\left[\frac{\bar{r}}{(1+\bar{r}^{-2n})^{1/n}}\right] \tag{2}$$

where r means non-dimensional radius based on the estimated core radius r_c . And the non-dimensional circulation Γ can be calculated by

$$\bar{\Gamma} = \int_0^{2\pi} V_\theta(r)\, r d\theta \tag{3}$$

In above equation the integration can be estimated by a simple relation with

$$\overline{\Gamma_e} = 2\pi r_c V_{\theta,peak} \tag{4}$$

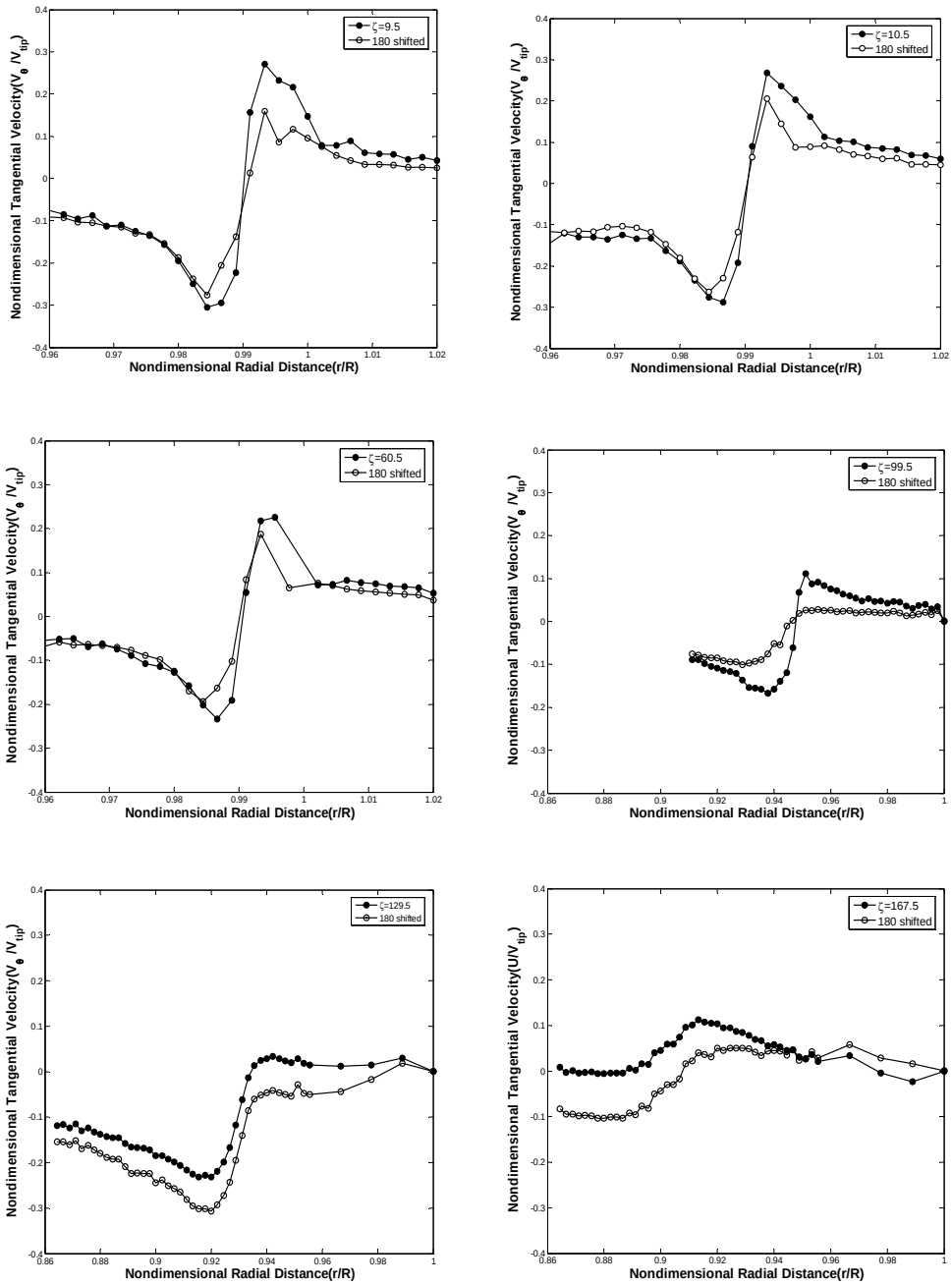

Fig. 6. Non-dimensional tangential velocity of tip vortices measured at wake ages of 9.5, 10.5, 60.5, 99.5, 129.5 and 167.5 degrees, appeared by solid symbols, and corresponded tip vortices generated by the other blade, shifted with 180 degrees, shown by void symbols

To assure the consistence of vortex evolution with wake age only tangential velocity components generated by new blade were chosen to apply model analysis and their results were plotted in the figure 7. As seen in the figure 7 experimental results are well matched to the n = 2 model specially in inbound region for all three wake ages while those of the outbound case were deviated by the reason of the helical trace as mentioned earlier.

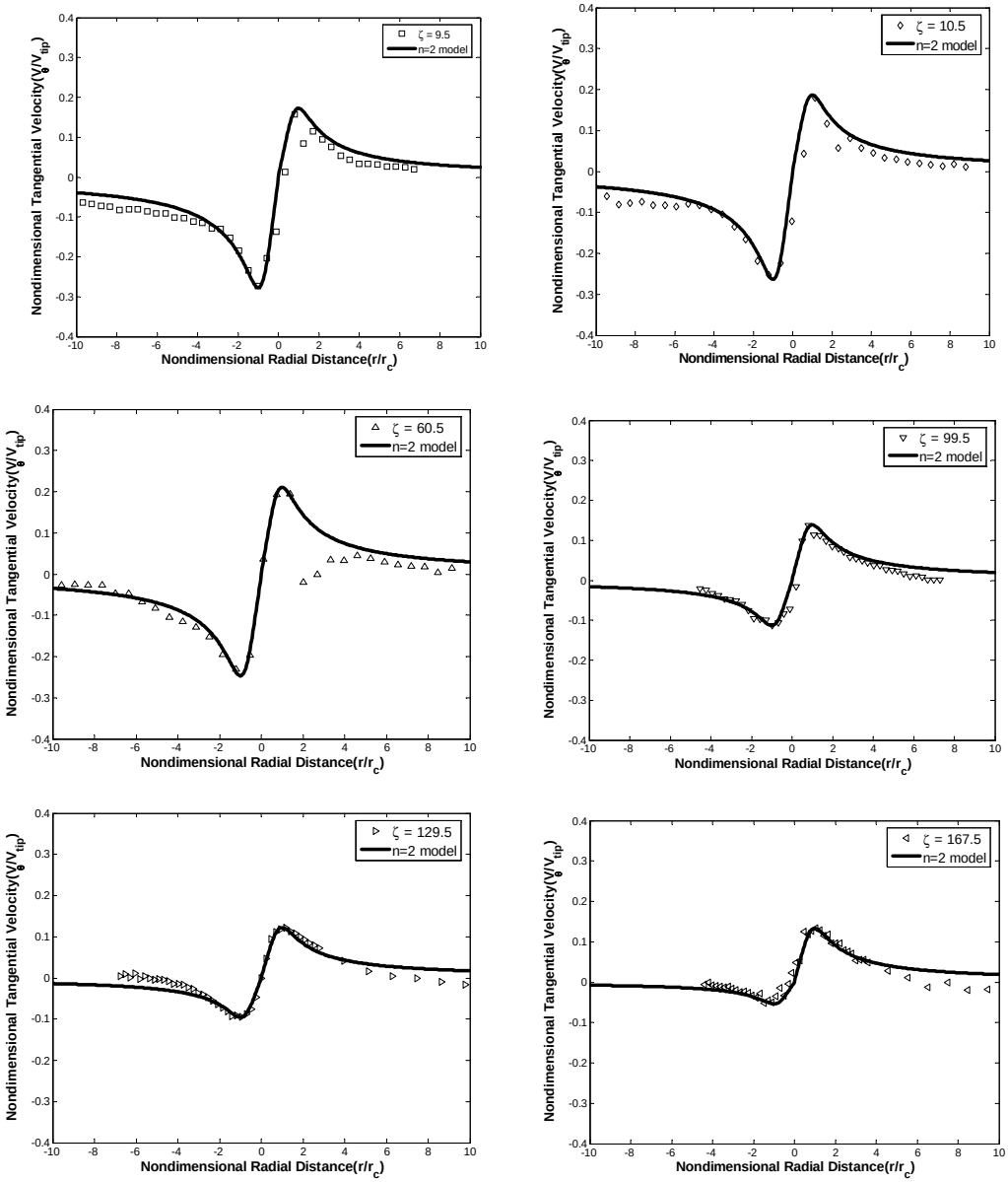

Fig. 8. Fitted profiles of tangential velocity components to Vatistas n=2 model for six different wake ages

Figure 8 was built by normalized values with both peaks of inbound and outbound of slipstream boundary. Results convince that tip vortices generated by two bladed rotor also undergo the laminar diffusion within a half of rotor revolution.

3.3 Vortex Core Growth

With refined profiles core radii were selected from calculated peaks to observe the core growth with wake age. For vortex core growth with wake age, the relation between vortex core radius and wake age are given as [1]

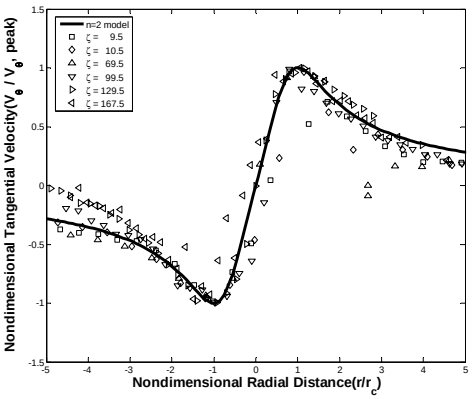

Fig. 9. Non-dimensional tangential velocities measured, and model profile based on Vatistas n=2 model of equation (2)

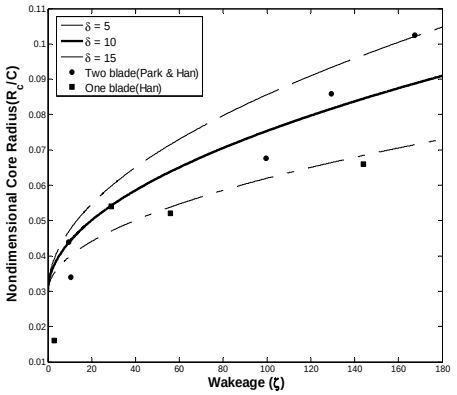

Fig. 10. Core growth with wake age

$$r_c(\zeta,\delta) = r_0 + 0.00855\sqrt{\delta\frac{\zeta}{\Omega}} \tag{5}$$

where r_0 is an initial core radius [m], δ is turbulent viscosity coefficient, Ω is rotor operation speed.

If an initial value of r_0 = 0.029 is used by extrapolating back to zero wake age, then it appears that a value of δ = 10 represents this viscous growth trend well. For the Han's one blade rotor [1], the rate of core growth appeared to be approximately the same, although the initial core size was somewhat large; one blade's initial core radius is 0.01. To permit a easier comparison, this plot shows both results and core growth curves δ = 5, 10 and 15, as given in figure 10

As seen in this figure tip vortex generated by two bladed rotor tends to diffuse slightly faster than the single blade case.

3.4 Axial velocities

The axial velocities in the vortex core were found to be small in magnitude relative to the tangential velocities, yet the results were noted to take on unique profiles, as shown in figure 11 which composes of only the selective wake ages; 9.5, 60.5 and 167 degrees to avoid redundancy with corresponded tangential velocities generated by other blade which are also shifted with 180 degrees. As seen in the tangential velocities the coincidence between axial velocity profiles of the first and the second blades was not accomplished, but the vortex diffusion can be easily examined quantitatively even with those raw data.

Another observation of axial velocity profiles also revealed that there were small but significant perturbations just outside the primary vortex core especially at 9.5, 60.5 wake ages. It may be clear the vortex wake generated by the second blade embedded inside the primary vortex. This is also different from the report done by Corsiglia et al [13]. They suggested that secondary vortices generated on rectangular rotor blade tips were affected, not by another blade wake.

As wake age grows the axial peak values at the core decrease drastically so that they become weak within a half revolution of the blade. Also the base width expands under diffusing process as shown in figure 11.

It is known that for a viscous laminar vortex, the axial velocity distributions are given by Lamb [14] as

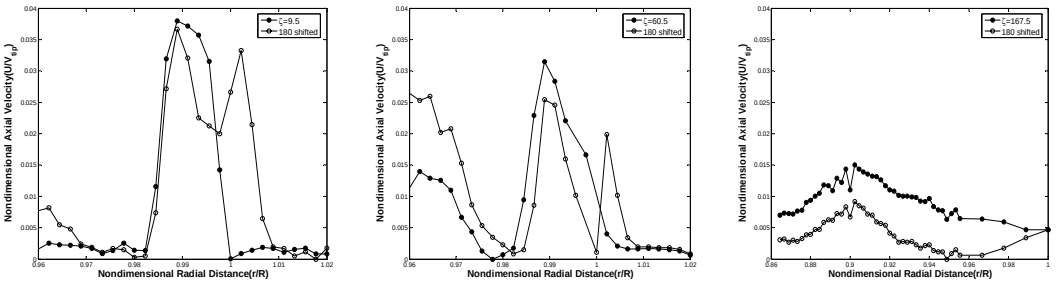

Fig. 11. Non-dimensional axial velocity profiles measured at three different wake ages, and shifted profiles made by other blade

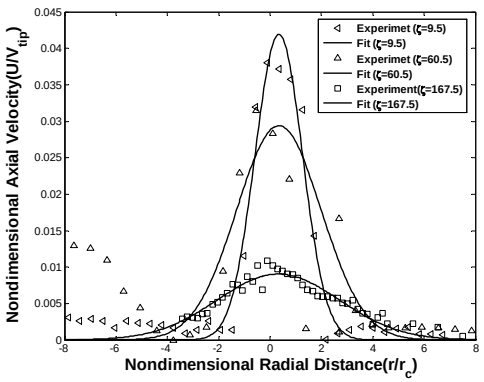

Fig. 12. Gaussian Curve fit of axial velocity at 9.5, 60.5 and 167.5 degrees of wake age

$$U(r,t) = \frac{A}{t}\exp(-\frac{r^2}{4\nu t}) \tag{6}$$

where A is a constant that can be related to the drag on the rotor blade [15]. Equation (6) is basically giving Gaussian profile in terms of the non-dimensional core radius. Results for those three cases are plotted in the figure 12.

The base width of fitted Gaussian curve shown in figures for the axial velocity profile mostly has ranged of two through six times of the vortex core radius for both sides. This base width explains how far the tip vortex flow spreads beyond the core radius. It is known that beyond the core region tip vortex flow experiences logarithmic region and outer region before dissipation starts [16]

3.5 Vortex Distortion

Fortunately, axial velocity profile of each tip vortices also contains information for the vortex distortion. Because the slip stream is contracted axial velocity profile becomes skewed to inboard direction as shown figure 13, normalized Gaussian profile. Skew rate explains how much the vortex distortion processed in terms of wake age, which may also be compared to those of the case of single blade. Figure 13 shows curve fit of axial velocity profile at wake age 9.5 degrees, and the skewness rate can be estimated by measuring the movement of center axis for this fitted curve, showing the trail formed rather inboard direction to the linear vortex trail which has the zero skewness and has Gaussian profile.

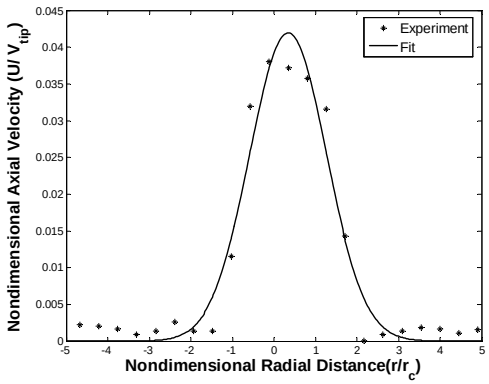

Fig. 13. Vortex distortion appeared in a skewed Gaussian fit for the axial velocity of 9.5 degrees of wake age

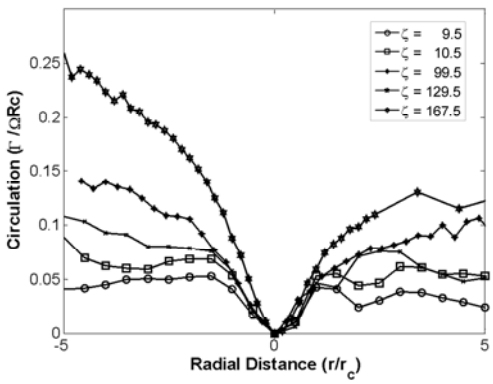

Fig. 14. Nomalized vortex circulations calculated by the equation (4)

Another observation for the vortex distortion can be made by vortex circulation. Vortex circulations were calculated by using the equation (5) for five wake ages as shown in the figure 14. As seen in this figure near the core circulation vortices were maintained as the certain level within these wake ages. As far as core circulation maintains with certain amount tip vortex stays on the diffusion only, but it is naturally expected that the distortion will starts when the core circulation starts to decay after a certain age. With measured data core circulation keeps on increasing. Therefore, more data in older wake age than 180 degrees are urgently needed.

Further analyses for the single blade rotor and their comparison with results of two bladed rotor have not gone through. It needs to examine the marginal distortion promoted by the second blade, but still above results could help describing the early distortion as well as vortex diffusion.

Still, it is very challenge to measure vortex velocity vectors shifted 180 degree of wake ages with such an experimental arrangement. Especially, to obtain the coincident data between two blades within one revolution seems to be real challenge. But it is observed that close data within 5 degrees could be accurate enough to examine objectives.

Conclusion

The tip vortex structure generated by two bladed model rotor system in a hover and its evolving behavior at three wake ages was examine using PIV system and 2-dimensional LDV system with tip Mach number of 0.27 and chord Reynolds number of 2.7 x 10^5. The following conclusions have been drawn from this work.

The slip stream formed by the two bladed rotor was contracted more drastically with a half revolution of the first rotor blade than the single case, and that its configuration was well matched to Landgrebe's model with $\lambda = 0.31$. And it was also found that the second blade promotes the tip vortex trail generated by the first blade to accelerate in downstream direction.

Tangential velocity component of tip vortex follows Vatistas' n=2 model within a reasonable accuracy especially in inbound region. Peak of tangential velocity at wake age of 99.5 degrees was reduced as much as a half in magnitude obtained at the wake age of 10 degrees. It implies that diffusion of tip vortex goes faster than that of single blade rotor.

Axial velocity profiles revealed that there were small but significant perturbations just outside the primary vortex core at three wake ages. It seems to be clear the vortex wake generated by the second blade embedded inside the primary vortex.

Acknowledgement

This work was supported by Agency for Defense Development and FVRC with Grant No. FVRC-V26. The program monitor was Dr. Sangho Kim, ADD. Authors gratefully acknowledge their supports.

References

1. Y. O. Han and J. G. Leishman, "Experimental Investigation of Helicopter Rotor Tip Vortex Alleviation Using a Slotted Tip Blade", *AIAA Journal*, Vol.42, No.3, pp. 523-535, March 2004.

2 F. H. Schmitz, *Rotor Noise, Aeroacoustics of Flight Vehicles: Theory and Practice*, Vol.1, NASA Reference Publication 1258, Aug. 1991, Chap.2.

3. S. Dawson, A. Hassan, F. Straub and H. Tadghighi, "Blade - Mounted Flap Control of BVI Noise Reduction Proof of Concept Test", *NASA Rept*. 195078, July 1995.

4 G. L. Crouse, J. G. Leishman and N. Bi, "Theoretical and Experimental Study of Unsteady Rotor/Body Aerodynamic interactions", *Journal of the American Helicopter Society*, Vol. 38, No. 1, 1992, pp. 55-64.

5 M. S. Torok and D. T. Ream, "Investigation of Empennage Airloads Induced by helicopter Main Rotor Wake", *American Helicopter Society 49th Annual Forum*, st. Louis, Mo, May 1993.

6 Y. O. Han and W. J. Chung, "Mean and turbulent characteristics if tip vortices generated by a slotted model blade", *5th international Symposium on Engineering Turbulence Modelling and Measurements,* September 16-18, Mallorca, Spain, 2002.

7 Y. O. Han, J. G. Leishman and A. J. Coyne, "Measurements of the Velocity and Turbulence Structure of a Rotor Tip Vortex," *AIAA Journal* Vol35, No3, pp. 477-485, 1997.

8 Y. O. Han "Diffused Tip Vortex Structure Generated by a Slotted Tip Rotor Blade," *The 43rd AIAA Aerospace Science Meeting and Exhibition*, AIAA Paper 2005-0057, Reno, NV. January 10-13, 2005.

9. A. J. Landgrebe, "The Wake Geometry of a Hovering Helicopter Rotor and its Influence on Rotor Performance", *Journal of the American Helicopter Society*, 17:4 pp. 2-15.

10. M. J. Bhagwat and J. G. Leishman, "Correlation of Helicopter Totor Tip Vortex Measurement", *AIAA Journal*, Vol.38, No.2, 2000, pp. 301-308.

11. A. Bagai, and J. G. Leishman, "A Study of Rotor Wake Development and Wake/Body interaction in Hover", *Journal of the American Helicopter Society*, Vol. 37, No. 4, 1992, pp. 48-57.

12. G. H. Vatistas, V. Kozel and W. C. Mih, "Simpler Model for Concentrated Vortices", *Experiments in Fluids*, Vol.24, No. 11, pp. 73-76.

13. V. R. Corsiglia, R.G. Schwind, And N. A. Chiglier, "Rapid Scanning Three-Dimensional Hot Wire Anemometer Surveys of Wing-Tip Vorices", *Journal of Aircraft*, Vol. 22, No. 2, 1985, pp. 158-160.

14. H. Lamb, *Hydrodynamics*, 6th end., Cambridge Univ. Press, New York, 1932, pp. 592, 593, 668, 669

15. A. Ogawa, *Vortex Flow*, Series on Fine Particle Science and Technology, CRC Press, Boca Raton, FL, 1993, pp. 193-196.

16. C. Tung, S. L. Pucci, F. X. Caradonna, and H. A. Morse, "The Structure of Trailing Vortices Generated by Model Rotor Blades", *Vertica*, Vol. 7, No.1, 1983, pp. 33-43.